Energy, Mines and Resources Canada
Énergie, Mines et Ressources Canada

CANMET

Canada Centre for Mineral and Energy Technology
Centre canadien de la technologie des minéraux et de l'énergie

Mining Research Laboratories
Laboratoires de recherche minière

LONG-LIVED RADIOACTIVE DUST CHARACTERIZATION IN URANIUM MILL OPERATIONS

J. BIGU (ELLIOT LAKE LABORATORY)

MRL 90-034 (TR) Dec. 1990

Canada

91-04538/

LONG-LIVED RADIOACTIVE DUST CHARACTERIZATION IN URANIUM MILL OPERATIONS

J. BIGU (ELLIOT LAKE LABORATORY)

MRL 90-034 (TR) Dec. 1990

33pp

MICROMEDIA

LONG-LIVED RADIOACTIVE DUST CHARACTERIZATION IN URANIUM MILL OPERATIONS

J. Bigu*

ABSTRACT

The characteristics of long-lived radioactive dust clouds generated in several mechanical and physico-chemical operations in a uranium mill have been investigated. The study consisted of the determination of dust size distribution, and of the size distribution of radionuclides associated with particulate matter in the size range <0.1 to 26 μm. Experiments were conducted using several cascade impactors operating at different sampling flow rates. Two different types of cascade impactors were used. Radionuclide identification was done using α-spectrometry and γ-spectrometry. Long-lived and short-lived radionuclides were identified in dust samples. The characteristics of the dust clouds depended on the mill operation. The following operations were studied: crushing (vibrating grizzly, jaw crusher, cone crusher); screening; ore transportation; grinding; acid leaching; counter-current decantation; yellowcake precipitation and drying; and yellowcake packaging. In addition, other dust and radioactivity measurements have been carried out.

Keywords: Long-lived radioactive dust; Uranium; Mine mill; Dust; Radioactivity.

*Research Scientist and Radiation/Respirable Dust/Ventilation Project Leader, Elliot Lake Laboratory, CANMET, Energy, Mines and Resources Canada, Elliot Lake, Ontario.

CARACTÉRISATION DES POUSSIÈRES RADIOACTIVES À PÉRIODE LONGUE DANS LES OPÉRATIONS D'USINES D'URANIUM

J. Bigu*

RÉSUMÉ

On a examiné les caractéristiques des nuages de poussières radioactives à période longue, qui sont produits dans une installation de traitement de l'uranium au cours de plusieurs opérations mécaniques et physico-chimiques. L'étude avait pour but de déterminer la répartition des poussières selon leur granulométrie et des radionucléides associées à des particules qui se trouvent dans l'intervalle de <0,1 à 26 µm. Les expériences ont été menées en utilisant plusieurs impacteurs à cascade qui fonctionnaient à différentes cadences d'échantillonnage. En fait, on a utilisé deux types d'impacteurs à cascade. On s'est servi de spectromètres alpha et gamma pour déterminer les radionucléides. L'étude d'échantillons de poussières a montré la présence de radionucléides à période longue et à période courte. Les caractéristiques des nuages de poussières sont fonction des opérations menées à l'installation de traitement. On a étudié les opérations suivantes : concassage (grille vibrante, concasseur à mâchoires, concasseur giratoire); criblage; transport du minerai; broyage; lixiviation acide; décantation à contre-courant; précipitation, séchage et emballage du concentré d'uranium. En outre, on a également effectué d'autres mesures des poussières et de la radioactivité.

Mots clés : poussières; poussières radioactives à période longue; radioactivité; uranium; usine de mine

*Chercheur scientifique et chef du projet sur les radiations/les poussières inhalables/la ventilation, Laboratoire d'Elliot Lake, CANMET, Énergie, Mines et Ressources Canada, Elliot Lake (Ontario).

INTRODUCTION

Inhalation of airborne radionuclides poses a potential health hazard to occupational workers in the nuclear industry. For this reason, monitoring of radioactivity concentration levels for dose exposure calculation purposes is a subject of considerable practical interest.

Some concern has recently been expressed with regards to the inhalation of respirable dust (approximate 1-10 μm size range) containing long-lived radioisotopes, as once inhaled and lodged in the respiratory system they will remain active as long as they are not eliminated by natural biological processes.

There is sparse information available regarding the long-term health effects of worker's exposure to long-lived radioactive dust (LLRD) such as that produced in underground uranium mine and uranium mill operations, nor is much data available on either LLRD chemical make-up or size distributions in uranium mines and mills. This information is important to identify the main radioisotopes in LLRD, their concentration in air, and their size distribution as the latter determines the LLRD deposition characteristics in the respiratory system.[1-3]

This paper presents experimental data collected in a uranium mill. Long-lived radioactive dust is generated in the course of mechanical and physico-chemical unit operations carried out in the separation and refining processes of uranium, or uranium chemical compounds, from uranium ores.

The data in this paper pertain to the main mechanical and physico-chemical milling operations. These include the following operations: ore transportation by conveyor belts, crushing, grinding, screening (i.e., sizing), acid leaching, counter-current decantation (CCD), solvent extraction, yellowcake precipitation, yellowcake drying and yellowcake packaging.

Measurements were conducted of LLRD and radon progeny associated with dust in the 1-30 μm size range, and radon progeny in the submicron size range. A variety of other dust and radioactivity measurements were also carried out.

EXPERIMENTAL APPARATUS AND METHODS

Size distribution analyses of radioactive dust, radioactive aerosol and dust were conducted by means of two 10-stage, radial slot-design, cascade impactors, model 210, manufactured by Sierra Instruments Inc. (U.S.A.), now Anderson. Depending on the particular application, the cascade impactors were operated with either 10 stages or 8 stages. In the latter case, the cascade impactors were operated with the last two ultrafine impactor stages removed. These two stages were eliminated at the expense of losing some size distribution information, but with the obvious benefit of substantially increasing the amount of dust collected on the remaining eight impactor stages.

Glass fiber filters (47 mm diameter), with radial slot design similar to that of the cascade impactor stages, were used as substrates to collect the samples. The cascade impactors were operated for about 12 hours at a time at a sampling flow-rate of 10.5 L/min (8-stage), and 3.3 L/min (10-stage).

The glass fiber substrates placed behind the stages of the cascade impactors enabled determination of the size distribution (mass median aerodynamic diameter (MMAD), and geometric standard deviation) of dust by determining the weight of the filters before and after the sampling period. Ambient temperature and pressure were carefully noted during sampling and results were corrected according to standard operating procedures. Total dust (mass concentration and activity concentration) was also estimated from cascade impactor data.

Radioactivity (α-particle) measurements on the impactor substrates also

enabled calculation of the long-lived radioactive dust (LLRD), and radon progeny, size distribution, i.e., activity median aerodynamic diameter (AMAD), and geometric standard deviation.

Also used in the determination of LLRD and radon progeny size distribution were two small, 8-stage, personal cascade impactors,[4] model Marple 298. These impactors differ significantly from the Sierra impactors in a number of ways such as size, weight and geometry. The Marple impactors are much smaller and lighter than the Sierra impactors. The impactor stages slot design is also different, i.e., six radial slots for the Marple impactor as opposed to four radial slots for the Sierra impactors. The Marple impactors were operated at a nominal flow-rate of 2 L/min. Stainless steel substrates were used as dust collectors. Because of the low flow rate at which these impactors are operated and the relatively large weight of the substrates, as compared with glass fiber filters, no attempt was made to measure dust, only the radioactivity associated with it.

The total LLRD and radon progeny concentrations were also estimated from impactor data. Radon progeny were measured 40 min after sampling. A counting time of 5 min was chosen. The α-particle activity of the LLRD was measured 1-2 weeks after sampling to allow the radon progeny and thoron progeny, if any, to decay away completely. Because of the low LLRD activity, each sample was counted several times for 30 min each time, and the average value, after subtracting the background, was used in the calculations.

The procedure used for the determination of dust, activity, and size distribution from the cascade impactor data was as follows:

1. Activity (dpm, i.e., disintegrations per min) and dust mass collected on each impactor stage were carefully noted.
2. Total activity and total dust mass from all the stages of the impactor, including the backfilter (BF), were measured.

3. Percentage (%) activity and % dust mass for each impactor stage were calculated.
4. Cumulative % of dust mass and cumulative % of activity, less than $D_{p,50}$ (see below), were estimated as follows. Dust mass (or activity) % of the BF was used as cumulative % for the last ultrafine stage. The cumulative % for the next stage was obtained by adding the % of dust mass (or activity) to the cumulative % dust mass (or activity) corresponding to the previous stage, and so on.
5. Cumulative % dust mass (or activity), less than $D_{p,50}$, versus EAD was plotted.

The variable $D_{p,50}$ is defined as the particle cut-off at 50% collection efficiency for spherical particles of density one. The magnitude EAD is the Equivalent Aerodynamic Diameter defined as the size of a spherical particle of density 1 g/cm^3 which has the same terminal settling velocity as the sampled particle.

In addition to cascade impactors, total dust mass in the respirable size range from ~1 μm to ~10 μm was monitored with a continuous, optical system, dust sampler model Mini-Ram PDM-3, manufactured by GCA (U.S.A.). Furthermore, respirable dust was measured using nylon cyclone samplers (cut-off size 3.5 μm). Total dust was determined by open-face filter techniques.

Identification of long-lived radionuclides was done using α- and γ-spectrometry of several dust samples. Spectrometric analyses were carried out using a silicon-barrier detector (SiBD) spectrometer for α-spectrometry, and a high purity Germanium detector (HPGD) for γ-spectrometry.

Dust generated by mechanical and physico-chemical operations in a uranium mill was sampled at several transfer points and locations in the mill. A brief description of the mechanical and physico-chemical operations of the mill are given below.

MECHANICAL OPERATIONS

Uranium ore from an ore pit and a nearby uranium mine was dumped by a truck loader into a piston-type rock breaker and a 'vibrating grizzly', where the ore was broken into smaller sizes and dropped into a chute which feeds a conveyor belt. Ore smaller than a given size was shaken directly into the chute. Sampling was done at the grizzly/conveyor belt transfer point which will be denoted hereafter as transfer point 1 (TP1).

Crushed ore from the grizzly was transferred to a jaw-crusher via a vibrating screen where finer ore drops through by-passing the second crushing operation. Coarser ore is further crushed to a smaller size by the jaw-crusher. Ore passing through the vibrating screen and the crusher is transported by a conveyor belt to special screens for size selection. Sampling in this area was done below the jaw-crusher feeding point, but above the transfer point onto the conveyor belt. This location will be denoted hereafter as transfer point 2 (TP2).

Ore from the jaw-crusher operation was fed onto a set of screens where the fines passed directly through to a conveyor belt and were stored in fine ore bins ready for grinding. The coarser ore was fed into a cone-crusher. Sampling was conducted in an area adjacent to the screens at the same level. This will be denoted as transfer point 3 (TP3).

Ore from the screens was further reduced in size by the cone-crusher and fed to a conveyor belt which was routed back to the screening operation. Sampling was carried out at the base of the cone-crusher, below and away from the feed point. This sampling location will be referred to as transfer point 4 (TP4).

Ore from the cone-crusher/screen system was delivered to the top of fine ore bins, for storage, by a 150 m long conveyor belt. The ore was then

fed from the base of the fine ore bins to the grinder for further ore size reduction. Sampling was done at the end of the long conveyor belt on top of the fine ore bins. This sampling location will be referred to as transfer point 5 (TP5).

Uranium ore was reduced to its final size by means of grinding with steel balls and cylinders. Sampling was conducted beside the grinder, i.e., transfer point 6 (TP6).

From the grinder onward the ore underwent a number of physico-chemical operations before its final processed stage in the mill, i.e., as yellowcake, and subsequent packaging in the packaging plant.

Several physico-chemical operations in the mill were monitored. Broadly speaking, this part of the mill circuit is as follows. The ground uranium ore from the rod and ball mills is treated with a neutral thickener. The neutral thickened slurry is treated with sulphuric acid, sodium chlorate and steam (acid leaching), and the leached slurry is directed to a series of counter-current decantation (CCD) tanks where the tailings are removed from the solution as a 55% solid slurry. Counter-current decant of the liquid solution, containing the uranium-rich phase, is fed to a clarification plant where the solution is passed through several sand filters to remove any suspended solid matter. The clarified liquid solution is directed to a liquid-liquid extraction plant. The effluent from the CCD is neutralized with milk of lime and removed from the plant to a tailings pond.

The filtered/clarified uranium-compound liquid phase solution is treated with a mixture of kerosene, alcohol and an amine. Kerosene is used as a liquid carrier. The alcohol is employed to keep the amine dispersed in the liquid phase. The amine reacts chemically with the uranium compound and forms an organic complex which is subsequently stripped from the liquid solution by means of sodium chloride. The scrubbed raffinate is treated with milk of lime

as indicated above.

The high grade uranium compound solution from the extraction process is treated with milk of magnesia where the uranium compound is precipitated as yellowcake. The yellowcake solution is thickened by settling and water evaporation. The yellowcake is dried in a dryer, stored in a yellowcake storage bin, and finally packaged in special drums in the yellowcake drying and packaging section for shipping and further processing and purification in the fuel fabrication cycle.

Monitoring was carried out on the following physico-chemical operations: acid-leaching, counter-current decantation, solvent extraction, and yellowcake precipitation and drying. The last mill operation, a mechanical operation, i.e., yellowcake packaging, was also monitored. Sampling at this location will be referred to as transfer point 7 (TP7). (It should be noted that the terminology 'transfer point' is only applied here to mechanical operations.)

Figure 1 shows a flow diagram of the mill where measurements were carried out. The flow diagram includes mechanical and physico-chemical operations.

EXPERIMENTAL RESULTS AND DISCUSSION

Measurements were conducted during March and June 1986. Four cascade impactors were used, namely: two Sierra impactors (Model 210) and two 8-stage Marple impactors (Model 298). During March, the Model 210 impactors were operated with 10-stages and 8-stages, respectively. During June, the two Sierra impactors were operated with 8-stages. Furthermore, the two Sierra impactors were located side by side at each sampling station during the March measurements. The purpose was twofold: to determine if the number of stages would affect the MMAD and AMAD, and to obtain two samples in the same location

for statistical purposes.

Because of the low sampling flow-rate of the Marple impactors, and the relatively low dust concentration in mill air at the time, no attempt was made to determine the dust mass on the different stages. Hence, no MMAD data from these impactors are available. Marple impactors were only used to gather radioactivity data to calculate the AMADs and the LLRD concentration in air.

Table I shows the average operating characteristics of the cascade impactors used. The table shows the operating sampling flow-rates and the corresponding cut-off sizes for each stage. The size range covered with these instruments was from about 0.06 μm to approximately 26 μm, depending on the number of stages and flow rates used.

The data obtained with the cascade impactors have been summarized in Tables II to IV, and Figures 2 to 5. These Figures show the percentage cumulative dust, and/or α-particle activity, versus EAD. (It should be noted that graphs for radon progeny are not shown here, but the data are plotted and the AMAD is calculated the same way as for the Long-Lived Radioactive Dust to which they are associated.) Figure 6 shows α-spectra for some samples. Table V shows total and respirable dust concentrations for several mechanical operations using open face filter holder samplers and nylon cyclones. Figure 7 shows dust concentration for several physico-chemical operations using an optical particle counter, Mini-Ram model PDM-3.

Tables II and III show cascade impactors data for long-lived radioactive dust (LLRD) and radon progeny. The data included are MMAD, AMAD, geometric standard deviations, dust concentration, LLRD concentration, and the specific radioactivity associated with dust. Tables II and III, and Figures 3 to 5 show the following features of practical interest:

1. The AMAD corresponding to the LLRD is, on average, larger than the corresponding MMAD of the carrier dust:

2. The MMAD decreases as the ore is crushed, screened and ground in the different mechanical operations in the mill. The MMAD follows the natural sequence of fragmentation from the vibrating grizzly to the grinding operations. The approximate range of values for the MMAD was 3 to 15 μm.
3. As for the MMAD, the values for the AMAD (LLRD) depended on the type of mechanical operation. The range of values found was approximately 3.7 to 19 μm.
4. The MMAD and AMAD corresponding to the last mechanical operation, in fact the last mill operation, namely, yellowcake packaging, were between the values corresponding to the vibrating grizzly and the jaw crusher.
5. Significant differences in the values of the MMAD were found in samples taken at the same location with impactors operated with different numbers or stages and air flows (12% to >50%). The same applies to the AMAD. There is no satisfactory explanation for the large discrepancy found between the Sierra and Marple cascade impactors data collected during the grinding operation. However, the data corresponding to the Sierra impactors are presumed to be more consistent with this milling operation.
6. As expected, the AMAD corresponding to the radon progeny associated with dust (not shown here) was much less than its corresponding MMAD. The AMAD obtained was in the range 0.15 to 0.7 μm, indicating that the radon progeny are preferentially associated with submicron particulate matter. The reader should be cautioned regarding the use of cascade impactors for radon progeny size distribution analysis for the reasons given below.

   The size of particles carrying radon progeny ranges from ~0.005 μm to ~0.2 μm. The number of radon progeny atoms borne by particles larger than 0.2 to 0.3 μm is negligible compared to the total number of aerosol particles. The small dimension of these particles makes them highly

susceptible to collection by diffusion as well as by impaction in cascade impactors. This phenomenon increases as the diameter decreases and makes the measurement of radon progeny size by cascade impactors difficult to interpret.

Measurement of fine particles ($\lesssim$0.3 μm) by cascade impactors is rather complex because of the difficulty in differentiating the contribution in the number of particles (or activity) collected on different stages by impaction from that due to diffusion. This is particularly true when the activity is the variable measured. When mass (or mass distribution) is the variable measured, biases introduced by the unwanted diffusion collection of fine particles is undetected on stages with a cut-off diameter larger than 0.5 μm because the mass of a particle varies with the cube of the diameter. The bias from fine particles would only be detected when the concentration is very high compared to that of larger particles (mixtures of mineral dust and diesel smoke for example)(see also reference 5).

7. No satisfactory explanation can be found at present for some significant differences in dust concentration measured in high dust-production areas of the mill by the Sierra and Marple cascade impactors placed side by side (see Table II). It should be noted that the dust concentration ratio between these two impactors is $\lesssim$2.0, whereas the ratio for their respective sampling flow-rates is about 3.2.
8. For the physico-chemical operations (see Table III), the largest values for AMAD and MMAD were found in the counter-current decantation (CCD), and yellowcake precipitation operations. Acid leaching and solvent extraction has lower values for the above variables, particularly solvent extraction.
9. As expected, the LLRD activity concentration was by far the highest for

the yellowcake packaging operation followed by yellowcake precipitation. Comparison of other mill operations is somewhat difficult because of the different air dilution factors between March and June. It should be noted that measurements of the mechanical operations were preferentially conducted during March, whereas monitoring of physico-chemical operations was carried out in June. For the mechanical operations, the highest LLRD concentration was found for yellowcake packaging (1.3×10^5 mBq/m^3) followed by crushing by the vibrating grizzly (1570 mBq/m^3). For the physico-chemical operations the highest LLRD concentration was obtained for the yellowcake precipitation followed by counter-current decantation and acid leaching (2110, 394, 252 mBq/m^3, respectively).

10. Total dust mass concentration ranged widely depending on the mill (mechanical) operations. It was highest at the vibrating grizzly and for the yellowcake packaging operations ($\geq$6 mg/m^3) followed by the jaw crusher ($\geq$1.5 mg/m^3). Dust concentration for the physico-chemical operations was lower than for the mechanical operation. Solvent extraction showed the lowest dust concentration.
11. Significant differences in the values of the AMAD were found in samples taken with the Sierra and Marple impactors. However, there are insufficient experimental data to quantify this statement unambiguously, and more work under controlled experimental conditions is necessary to compare the performance of the two types of impactors.
12. Radioactivity measurements of the dust collected on cascade impactor substrates show that gross α-activity was not always linearly proportional to the amount of dust collected on the impactor substrates. It was found that the ratio of α-activity to dust mass decreased as the latter increased. These results suggest significant α-particle absorption in dust. From these data it may be concluded that although

relatively high dust mass is preferable to low dust mass for MMAD calculations, this may lead to substantial uncertainties in the determination of the AMAD. As discussed later, the actual α-activity measured on each stage should be verified by liquid scintillation counting of the same samples, or by neutron activation analysis.

It is presumed that the contribution to the LLRD concentration (mBq/m^3) and its specific concentration (mBq/mg), from some cascade impactor stages, may have been underestimated for mill operations that generated substantial amounts of dust. Self-absorption problems can be minimized by choosing sampling times to ensure that adequate amounts of dust will be collected for accurate MMAD determination, while at the same time consistent with low α-particle absorption necessary for reliable measurements of the AMAD. It should be noted that during March, dust concentrations were much higher than in June when doors and windows remained open day and night.

It should be noted that the specific activity for the yellowcake precipitation operation calculated from data obtained in March and June differed by a factor of 10 to 14. This large difference can be attributed to differences in the grade of processed ore, and to 'cleaner' practices during June, e.g., open doors and the like. The former supposition was later confirmed by mill personnel, i.e., the grade of the ore processed in June was much lower than the grade processed in March. Notice that the specific activities for the two experimental runs on March were quite close and within experimental error. The same applies to the two runs in June, with somewhat larger differences. These data indicate that the grade of the ore was constant for each case, e.g., March and June, although much higher for March.

Table IV shows average values of MMAD and AMAD calculated from data in Tables II and III for the mill operations investigated.

Identification of the radionuclides in the radioactive dust was done by means of α-spectrometry and γ-spectrometry (see Fig. 6).

Alpha-spectrometry on at least one sample of each mechanical and physico-chemical operation was carried out under vacuum conditions in order to improve the energy resolution of the spectra. Except for yellowcake samples, counting times in excess of 24 hours were necessary for good counting statistics.

Because of (a) self-absorption effects, i.e., α-particle absorption in dust, leading to spectrum broadening and photopeak overlapping; (b) relatively low signal-to-noise ratio; and (c) spectrometer drift, positive identification of the radionuclides in dust samples by α-spectrometry was not straightforward. A ^{241}Am source and a $^{226}Ra/^{232}Th$ source were used before and after each radioactive measurement of each dust sample. The above radioactive sources provided the following α-energy lines for α-particle identification and α-spectrometer calibration purposes:

$$^{241}Am : \bar{E}_\alpha = 5.45 \text{ MeV}$$

$$^{218}Po : \bar{E}_\alpha = 6.0 \text{ MeV}$$

$$^{214}Po : \bar{E}_\alpha = 7.69 \text{ MeV}$$

$$^{212}Po : \bar{E}_\alpha = 8.78 \text{ MeV}$$

Analysis of the data from mechanical operations samples showed three main photopeaks with the following α-particle average energies: 4.13 ± 0.22 MeV, 4.75 ± 0.32 MeV, and 7.17 ± 0.3 MeV, which can tentatively be ascribed to ^{238}U (4.3 MeV), ^{226}Ra (4.8 MeV) and ^{214}Po (7.69 MeV).

Identification of the high energy α-particle peak was difficult because of spectral broadening and poor statistics of counting. The contribution from ^{222}Rn (5.48 MeV) and ^{218}Po (6.00 MeV) in the samples to the α-spectrum could not be ascertained because of photopeak broadening and overlapping.

Alpha-spectra analyses from physico-chemical operations and yellowcake packaging showed two main photopeaks with the following energies: 3.99 ± 0.13 MeV and 4.46 ± 0.18 MeV. These two photopeaks can tentatively be ascribed to ^{238}U (4.2 MeV) and $^{234}U/^{230}Th$ (4.7 MeV). The lower α-particle energy measured for these radioisotopes is attributed to energy degradation in dust, i.e., self-absorption. Only these two peaks appear in the spectra corresponding to yellowcake precipitation, solvent extraction and yellowcake packaging. Counter-current decantation and acid leaching spectra also show a much smaller photopeak of higher energy which could not be unambiguously identified.

The radioisotope identification indicated above assumes little or no thorium present in the dust samples. This assumption is supported by open-face radon progeny grab-sampling measurements 40 min and 7 h after sampling. These measurements showed negligible residual α-activity after the radon progeny decayed away.

Figure 6 shows α-particle spectra corresponding to three different mill operations, namely: cone crushing, yellowcake precipitation and yellowcake packaging. The difference in photopeak α-energy location is ascribed, as indicated above, to self-absorption.

Dust samples from all the mill mechanical operations were analyzed by γ-spectrometry. However, despite the very high resolution of the apparatus (0.5 keV/channel), positive identification of the radionuclides in the dust samples was rather difficult even after counting for extended periods. The reason for this is the low radioactivity in the samples and the relatively large natural background. (The activity of the samples is related to the sampling time which determines the amount of dust collected at a given flow-rate, and the ore grade.) Although many peaks were found in the samples, only the radioisotopes ^{214}Pb and ^{210}Pb could be identified with reasonable certainty as belonging to the samples and not to background.

Because of the relatively large amount of dust generated in yellowcake packaging, the activity of the samples from this operation was easily measurable and the radioisotope make-up could be quite confidently identified. The following radioisotopes were identified: ^{234}Th, ^{234m}Pa, ^{234}U, ^{230}Th and some ^{226}Ra, ^{210}Pb and ^{235}U. The radioisotope composition for physico-chemical operations was somewhat similar but the activity considerably smaller, a fact that made identification somewhat difficult at times.

Table V shows total and respirable dust measurements for several mechanical operations. Measurements were conducted using open-face filter and nylon cyclone samplers. The values for total dust are in fair agreement with data using the cascade impactors (see Table II). Respirable dust concentrations were, of course, substantially lower than total dust concentration.

Figure 7 shows the respirable dust concentration (mg/m^3) measured during several physico-chemical operations with a real-time, passive, continuous dust monitor (model Mini-Ram PDM-3 manufactured by GCA U.S.A.). Three operations were monitored: counter-current decantation, acid leaching and yellowcake precipitation. The dust concentration was highly variable but was in general below 1 mg/m^3. The lowest dust concentration was found in yellowcake precipitation. Apart from the three operations indicated above, no other physico-chemical operations were monitored with this instrument.

SUMMARY AND CONCLUSIONS

From this study the following conclusions can be drawn. The AMAD corresponding to the long-lived radioactive dust was, in general, slightly larger than the corresponding MMAD of the carrier dust.

The MMAD and AMAD calculated for the dust cloud depended on the type of mechanical and physico-chemical operations in the mill. The values for these

:wo diameters were in the range 3 to 19 μm.

The AMAD corresponding to the radon progeny was in the submicron range, i.e., 0.11 to 0.7 μm. It should be indicated that the AMAD corresponding to the radon progeny is best measured using diffusion batteries. Hence, the data presented here obtained with cascade impactors are assumed to be accurate (at best) to a first approximation only. The reason for using cascade impactors is simply that they were available for LLRD measurements.

Differences were found for the MMAD and AMAD obtained at the same location with different types of cascade impactors, or using the same kind of impactors but sampling under different operating conditions. It is suggested that this topic should be further investigated.

The long-lived radioactive dust concentration depended on the mechanical operation. It was highest for the grizzly (TP1), and yellowcake packaging (TP7) operation, followed by some crushing operations, e.g., jaw-crusher (TP2).

Alpha-particle self-absorption, i.e., absorption in dust, was a problem for some samples when the mass collected in some impactor stages, in certain mechanical operations, was higher than a critical value. Hence, errors should be minimized by choosing sampling times consistent with adequate dust mass collection for accurate calculation of the MMAD, and low α-particle self-absorption for precise determination of the AMAD. Alternatively, use could be made of liquid scintillation counting and/or neutron activation analysis.

Identification of radionuclides by α-spectrometry and γ-spectrometry was not straightforward, except for yellowcake packaging, because of the low specific activity of some of the samples. Some of the following radionuclides were tentatively identified depending on the sample, i.e., mill operation: ^{238}U, ^{226}Ra, ^{234}U, ^{230}Th, ^{235}U, ^{234m}Pa, ^{234}Th, ^{214}Po, ^{214}Pb and ^{210}Pb.

Knowledge of the AMAD and LLRD radionuclide composition permits the

estimation of some important health risk indices and radiation exposure variables such as the annual limit of intake (ALI).

ACKNOWLEDGEMENTS

This study was requested and partly supported by Atomic Energy Control Board (AECB). The authors would like to acknowledge the technical assistance of E. Edwardson in conducting experimental work and assisting in some calculations. The authors would also like to thank Mr. T. Meadley (AMOK Ltd., Saskatoon) for his cooperation throughout this study. Finally, the authors would like to acknowledge the assistance of some of the staff at Cluff Lake Mining during this field investigation.

REFERENCES

1. Bigu, J. and Grenier, M.G., "Studies of Radioactive Dust in Canadian Uranium Mines". CIM Bull. 77:62-68 (1984).

2. Duport, P.J. and Edwardson, E., "Characterization of Radioactive Long-Lived Dust Present in Uranium Mine and Mill Atmospheres". In Proc Occup Radiation Safety in Mining, vol. 1. Edited by H. Stocker. Toronto: Canadian Nuclear Association, 1985, pp. 189-195.

3. Bigu, J. and Grenier, M.G., "Characterization of Radioactive Dust in Canadian Underground Uranium Mines". In Proc 2nd Ventilation Congr.. Edited by P. Mousset-Jones. Reno (Nevada), A.A. Balkema, Rotterdam. 1985, pp. 269-277.

4. Hinds, W.C., Liu, W.V. and Froines, J.R., "Particle Bounce in a Personal Cascade Impactor". Am Ind Hyg Assoc J. 46:517-523 (1985).

5. Barzic, J.Y., "Etude de l'aerosol d'une mine d'uranium". Ph.D. Thesis. L'Universite de Bretagne Occidentale (France), 1975.

Table I - Cascade impactors operating characteristics

Impactor	Sampling Flow-Rate L/min	Stage Number	Cut-Off Size µm
Sierra* (Model 210)	3.3	1	26
		2	16
		3	6.4
		4	3.8
		5	2.5
		6	1.4
		7	0.8
		8	0.5
		9	0.3
		10	0.06
Sierra (Model 210)	10.5	1	14.8
		2	8.8
		3	3.5
		4	2.1
		5	1.4
		6	0.8
		7	0.4
		8	0.23
Marple (Model 298)	2.0	1	21.3
		2	14.8
		3	9.8
		4	6.0
		5	3.5
		6	1.55
		7	0.93
		8	0.52

*In June. this impactor was operated at a sampling flow rate of 10.5 L/min. The cut-off sizes for this case are the same as those corresponding to the other Sierra impactor.

Table II - Cascade impactors data for several mechanical operations in a uranium mill

Mechanical Operation	Date 1985	Impactor	MMAD µm	Dust σg	AMAD(LLRD) µm	LLRD σg	AMAD(RnD) µm	RnD σg	Dust Conc. mg/m^3	LLRD Conc. mBq/m^3	LLRD(S.A.) mBq/mg
Grizzly (TP1)	March 22	S1	15.4	2.8	15.3	3.4	0.66	9.1	12.51	1090	87
		S2	14.5	2.4	19.0	3.0	0.69	2.6	8.99	1570	175
Jaw Crusher (TP2)	March 23	S1	12.8	3.0	12.3	3.3	0.26	6.5	2.70	380	141
		S2	8.4	2.7	7.6	3.7	0.16	13.6	1.53	380	248
Cone Crusher (TP4)	March 25	S1	5.4	2.6	5.7	2.8	-	-	0.84	190	226
		S2	6.6	2.4	6.2	3.4	-	-	0.86	270	314
Screens (TP3)	March 24	S1	5.3	2.3	5.8	2.6	0.58	4.7	1.69	390	231
		S2	6.2	2.4	5.7	3.0	0.69	4.6	1.49	520	349
Top Fine Ore Bin/ Conveyor Belt #8 (TP5)	March 26	S1	4.0	3.3	4.0	3.3	0.31	7.1	0.30	180	600
		S2	3.7	4.5	4.1	3.5	0.14	13.6	0.37	230	605
	June 8	S2	3.4	2.8	3.8	3.1	-	-	0.08	100	1250
Grinding (TP6)	June 5	S2	-	-	3.7	5.8	0.20	10.5	-	48	-
	June 7	M_2	-	-	10.0	2.3	-	-	-	59	-
Yellowcake Packaging (TP7)	March 22	S1	10.5	3.1	11.1	3.5	-	-	12.43	1.3×10^5	1.05×10^4
		S2	12.3	3.7	11.8	2.6	-	-	6.21	1.25×10^5	2.01×10^4

Notes: a) S1 and S2 are Sierra impactors. M_2 is a Marple impactor.
b) σg represents geometric standard deviation (µm).
c) RnD stands for radon progeny.
d) S.A. indicates specific activity.

Table III - Cascade impactors data for several physico-chemical operations in a uranium mill

Operation	Date	Impactor	MMAD (μm)	Dust σg	AMAD(LLRD) (μm)	LLRD σg	AMAD(RnD) (μm)	RnD σg	Dust Conc. mg/m³	LLRD Conc. mBq/m³	LLRD(S.A.) mBq/mg
Acid Leaching	June 5	S1	6.9	2.4	6.6	3.5	0.24	4.0	0.30	252	840
	June 7	S1	7.4	2.8	9.5	4.0	0.17	4.2	0.23	181	787
Counter-Current Decantation (CCD)	June 7	S2	8.3	3.0	10.2	3.6	0.21	3.0	0.40	266	665
	June 5	M_1	-	-	12.8	1.7	0.15	33.0	-	394	-
	June 5	M_2	-	-	10.5	1.8	0.33	16.0	-	371	-
	June 6	M_1	-	-	13.1	1.8	0.11	14.7	-	160	-
Solvent Extraction	June 6	S2	4.5	5.3	2.9	3.7	0.40	3.3	0.06	39	650
	June 6	M_2	-	-	3.8	3.9	0.58	2.8	-	31	-
Yellowcake Precip.	March 27	S1	7.0	4.0	16.2	3.8	0.27	5.0	0.34	2110	6206
	March 27	S2	9.0	2,8	13.2	3.6	0.18	8.3	0.31	1890	6097
	June 8	S1	5.4	6.3	9.0	4.7	-	-	0.30	134	447
	June 7	M_1	-	-	13.2	1.8	-	-	-	106	-
	June 6	S1	4.0	3.8	6.6	4.9	0.40	10.8	0.06	35	583
Yellowcake Packaging	March 22	S1	10.5	3.1	11.1	3.5	-	-	12.43	1.30×10^5	1.05×10^4
	March 22	S2	12.3	3.7	11.8	2.6	-	-	6.21	1.25×10^5	2.01×10^4

Notes: a) S1 and S2 are Sierra impactors; M_1 and M_2 are Marple impactors.
b) σg represents geometric standard deviation.
c) RnD stands for radon progeny.
d) S.A. indicates specific activity.
e) Yellowcake packaging data have been included for completeness.

Table IV - Average values of MMAD and AMAD for different mill operations.

Mill Operation	MMAD μm	AMAD μm
Grizzly	14.95	17.15
Jaw Crusher	10.60	9.95
Cone Crusher	6.00	5.95
Screens	5.75	5.75
Ore Bin/Conveyor Belt	3.70	3.97
Grinder	-	6.85
Acid leaching	7.15	8.05
CCD	8.3	11.65±1.51
Solvent extraction	4.5	3.35
Yellowcake precipitation	6.35±2.15	11.64±3.8
Yellowcake packaging	11.4	11.45

Table V - Total and respirable dust concentration during some milling mechanical operations.

Location	Total Dust[1] (mg/m^3)	Respirable Dust[2] (mg/m^3)
Jaw crusher (TP2)	2.16	0.28
Screens (TP3)	1.58	0.41
Cone crusher (TP4)	0.83	0.11
Conveyor belt/ Fine ore bin (TP5)	0.23	0.16

[1] Using an open-face filter holder.

[2] Using a nylon cyclone.

LIST OF ILLUSTRATIONS

Figure 1. Block diagram of mechanical and physico-chemical operations in a uranium mill.

Figure 2. Percentage cumulative dust versus EAD for the grizzly/crusher fragmentation operation (measurements made with two cascade impactors).

Figure 3. Percentage cumulative LLRD α-particle activity versus EAD for the screening operations (measurements conducted with two cascade impactors).

Figure 4. Percentage cumulative dust (MMAD), and percentage cumulative LLRD α-particle activity (AMAD), versus EDA for the solvent extraction operations.

Figure 5. Percentage cumulative dust (MMAD), and percentage cumulative LLRD α-particle activity (AMAD), versus EDA for the yellowcake precipitation operation.

Figure 6. Alpha-particle spectra corresponding to different mill operations.

Figure 7. Dust concentration for several physico-chemical operations.

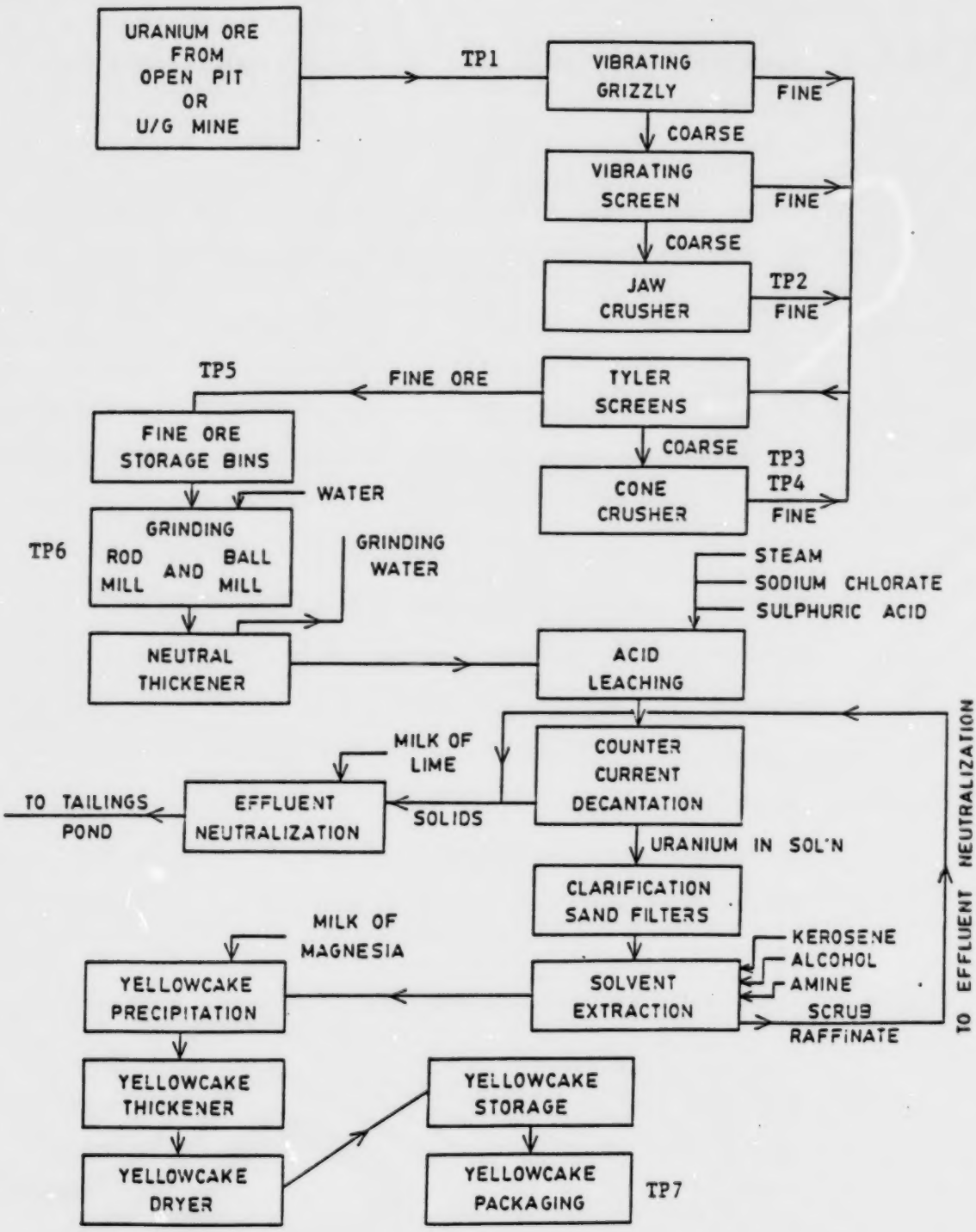
URANIUM ORE FROM OPEN PIT OR U/G MINE
TP1
VIBRATING GRIZZLY
FINE
COARSE
VIBRATING SCREEN
FINE
COARSE
JAW CRUSHER
TP2
FINE
TP5
FINE ORE
TYLER SCREENS
FINE ORE STORAGE BINS
COARSE
TP3
TP4
CONE CRUSHER
FINE
WATER
GRINDING ROD AND BALL MILL
TP6
GRINDING WATER
STEAM
SODIUM CHLORATE
SULPHURIC ACID
NEUTRAL THICKENER
ACID LEACHING
MILK OF LIME
COUNTER CURRENT DECANTATION
TO TAILINGS POND
EFFLUENT NEUTRALIZATION
SOLIDS
URANIUM IN SOL'N
CLARIFICATION SAND FILTERS
MILK OF MAGNESIA
KEROSENE
ALCOHOL
AMINE
YELLOWCAKE PRECIPITATION
SOLVENT EXTRACTION
SCRUB
RAFFINATE
TO EFFLUENT NEUTRALIZATION
YELLOWCAKE THICKENER
YELLOWCAKE STORAGE
YELLOWCAKE DRYER
YELLOWCAKE PACKAGING
TP7

Figure 1

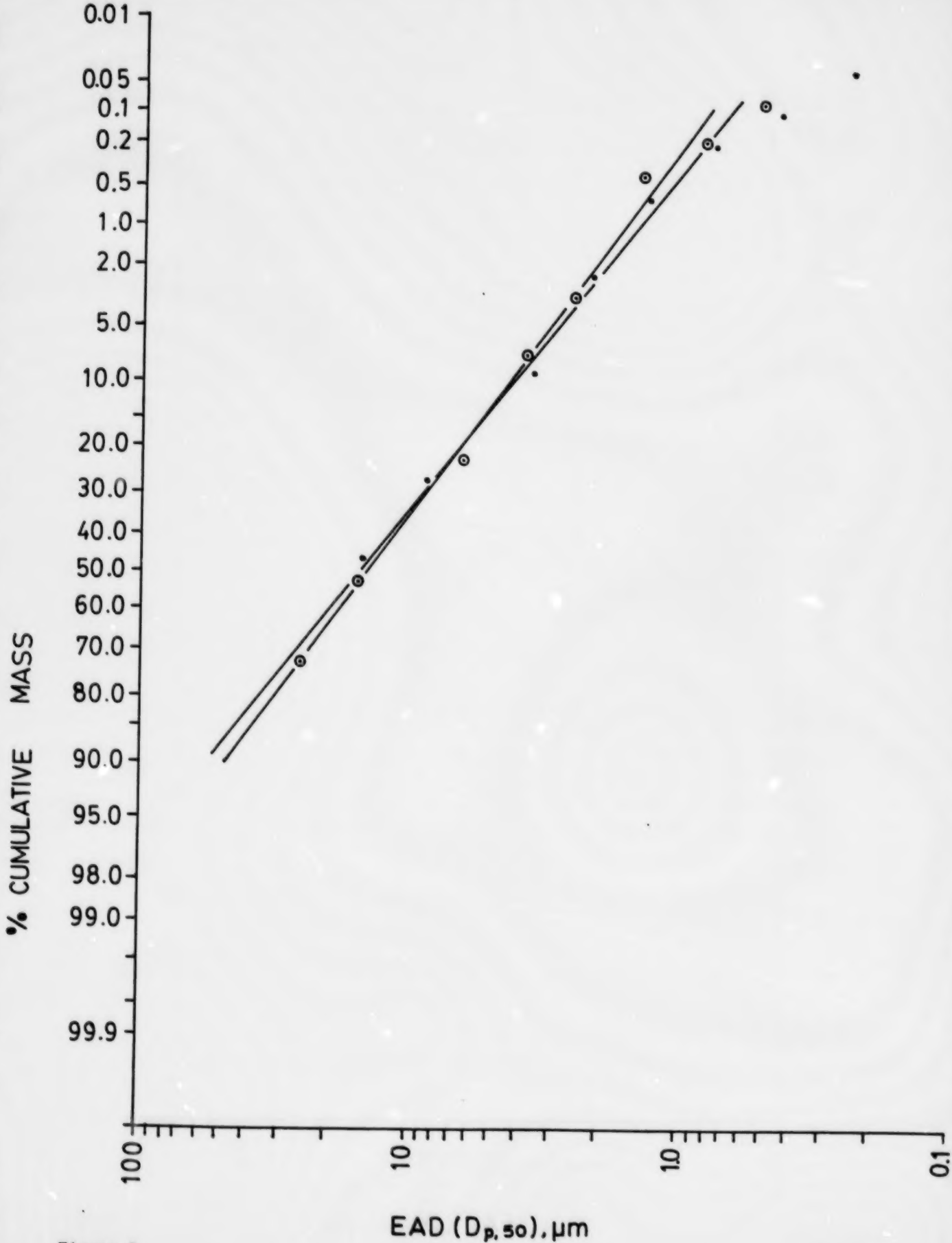
0.01
0.05
0.1
0.2
0.5
1.0
2.0
5.0
10.0
20.0
30.0
40.0
50.0
60.0
70.0
80.0
90.0
95.0
98.0
99.0
99.9
% CUMULATIVE MASS
100
10
1.0
0.1
EAD ($D_{p,50}$), µm

Figure 2

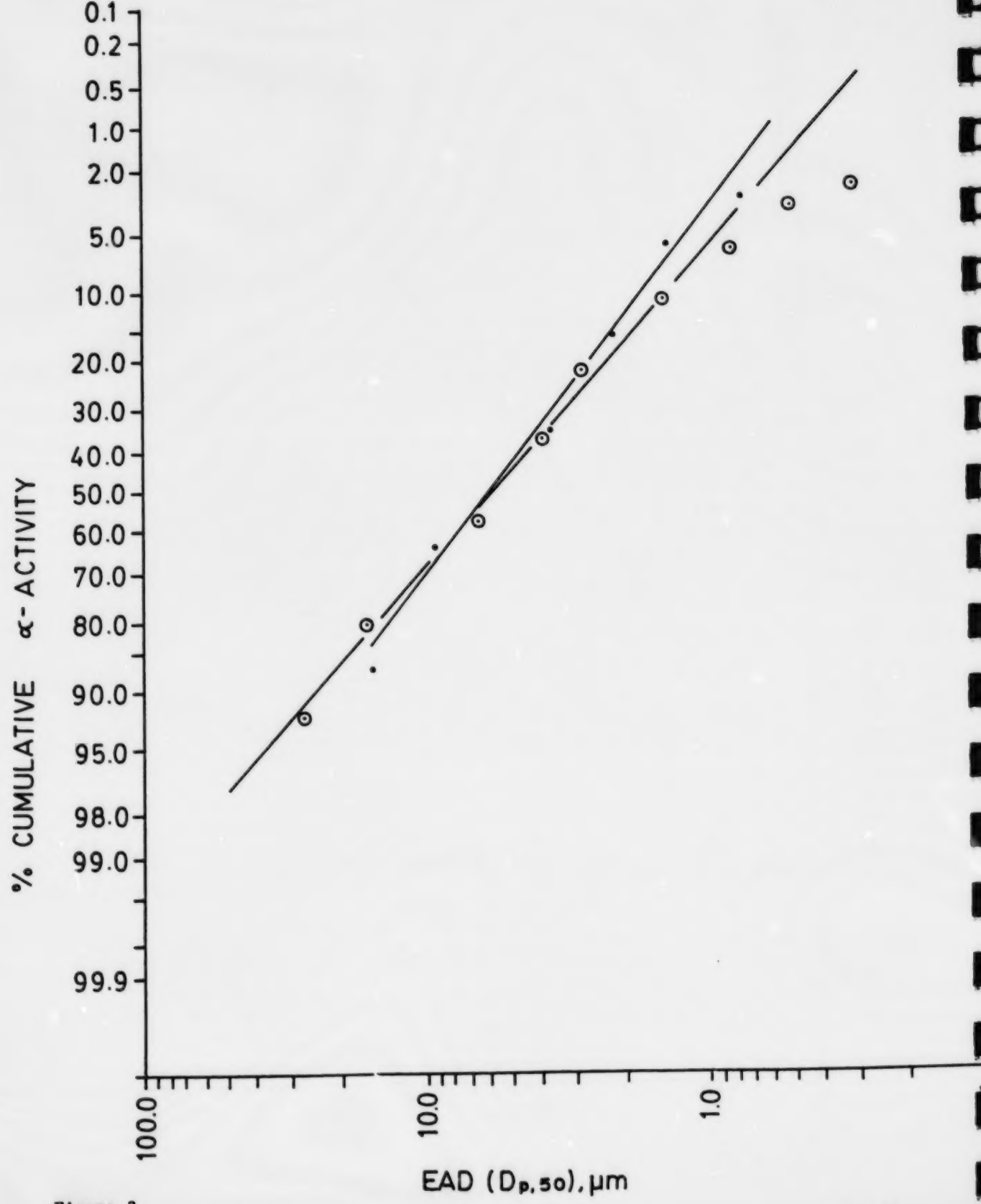
0.1
0.2
0.5
1.0
2.0
5.0
10.0
20.0
30.0
40.0
50.0
60.0
70.0
80.0
90.0
95.0
98.0
99.0
99.9
% CUMULATIVE α- ACTIVITY
100.0
10.0
1.0
EAD (Dp,50), µm

Figure 3

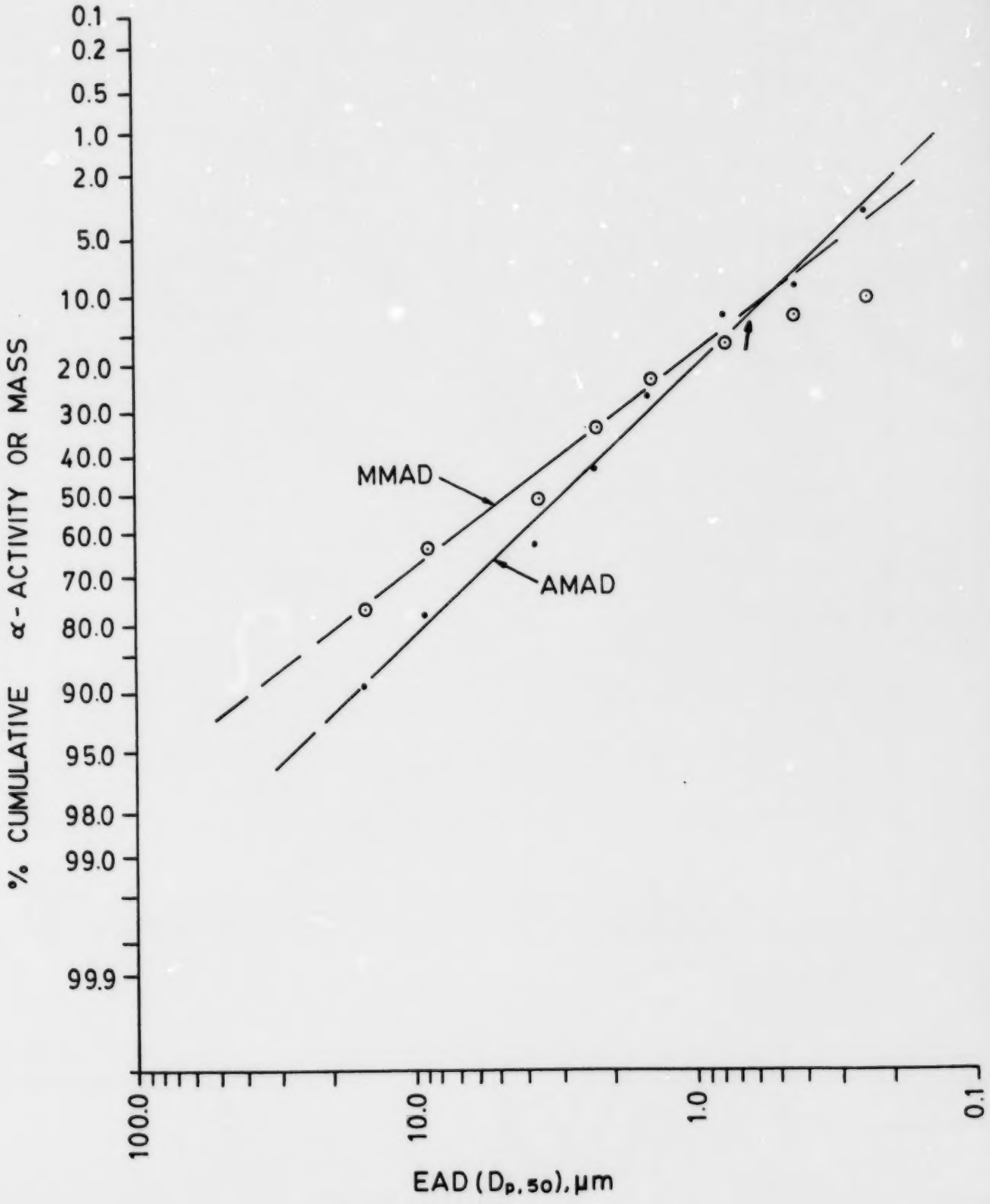
0.1
0.2
0.5
1.0
2.0
5.0
10.0
20.0
30.0
40.0
50.0
60.0
70.0
80.0
90.0
95.0
98.0
99.0
99.9
% CUMULATIVE α-ACTIVITY OR MASS
MMAD
AMAD
100.0
10.0
1.0
0.1
EAD (Dp,50), µm

Figure 4

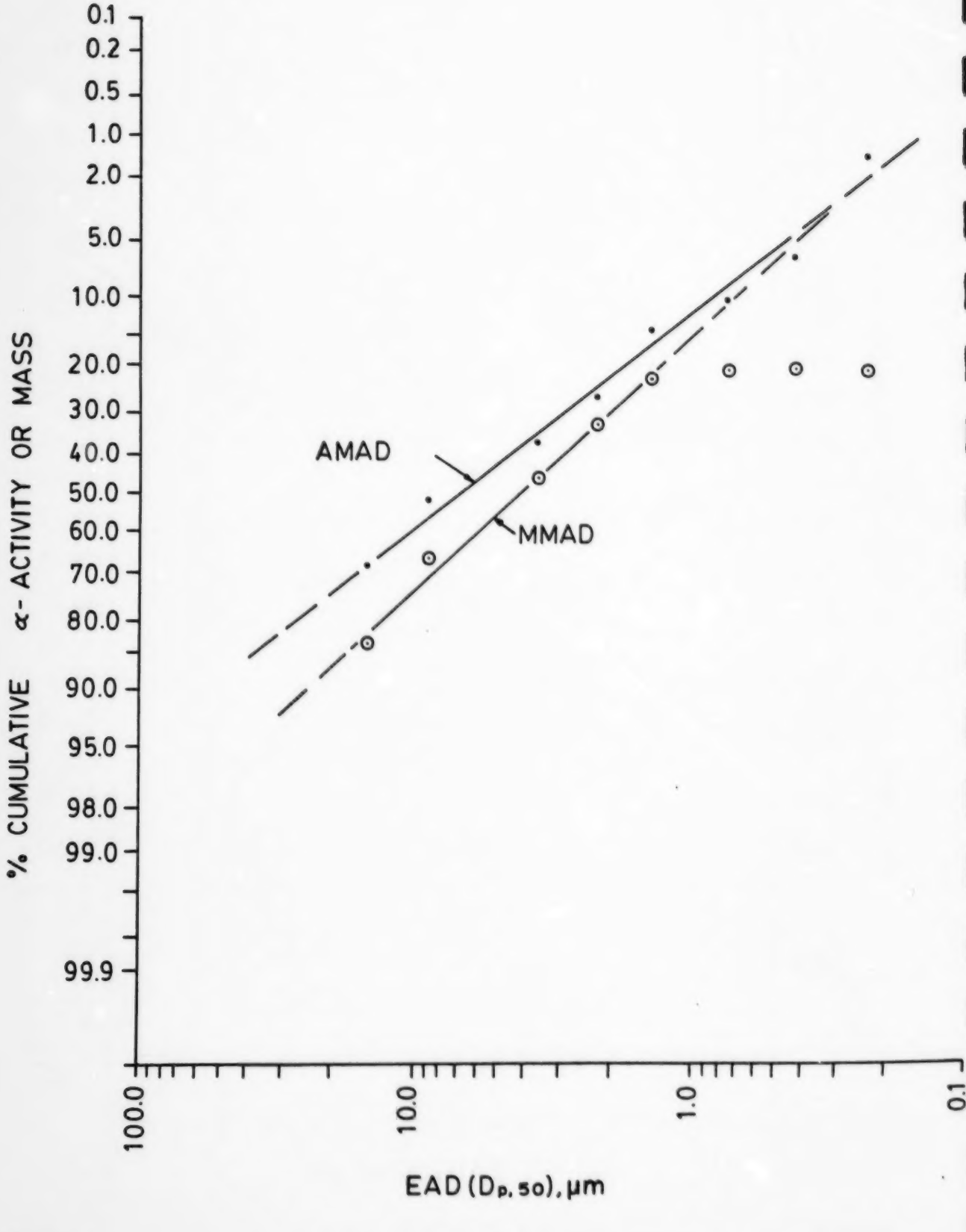
0.1
0.2
0.5
1.0
2.0
5.0
10.0
20.0
30.0
40.0
50.0
60.0
70.0
80.0
90.0
95.0
98.0
99.0
99.9
% CUMULATIVE α- ACTIVITY OR MASS
AMAD
MMAD
100.0
10.0
1.0
0.1
EAD (Dp, so), μm

Figure 5

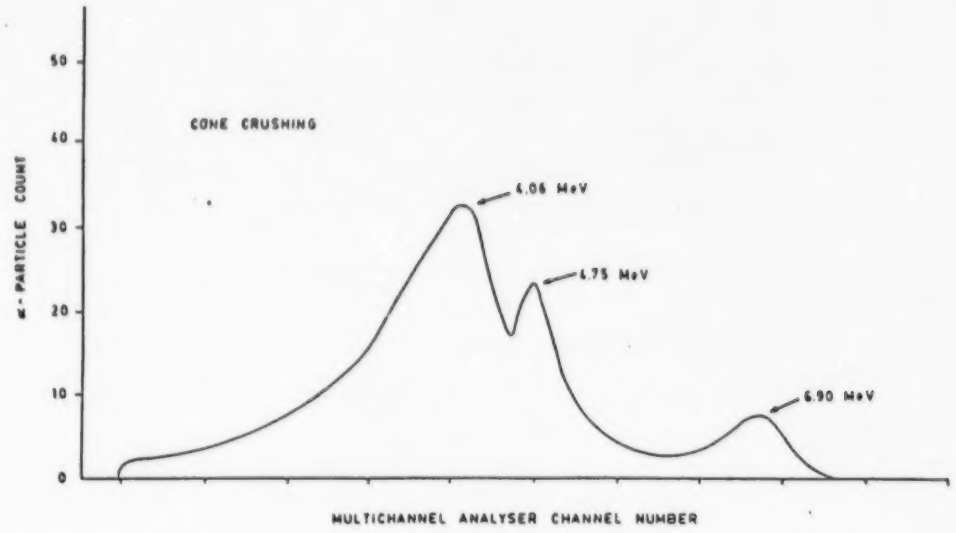
CONE CRUSHING
4.06 MeV
4.75 MeV
6.90 MeV
α - PARTICLE COUNT
MULTICHANNEL ANALYSER CHANNEL NUMBER

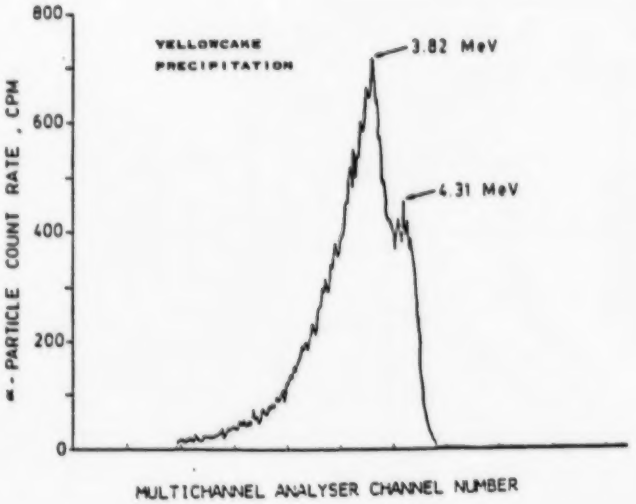
YELLOWCAKE PRECIPITATION
3.82 MeV
4.31 MeV
α - PARTICLE COUNT RATE , CPM
MULTICHANNEL ANALYSER CHANNEL NUMBER

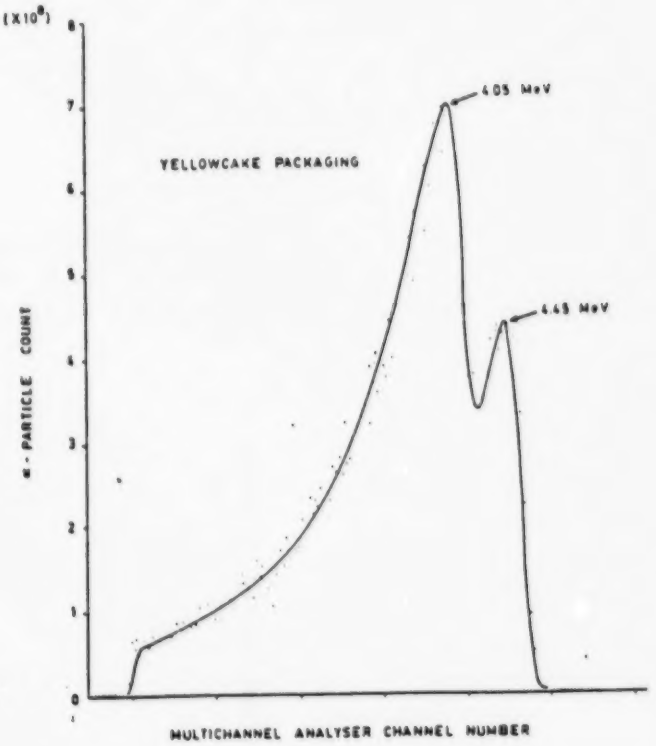
(X10⁶)
YELLOWCAKE PACKAGING
4.05 MeV
4.43 MeV
α - PARTICLE COUNT
MULTICHANNEL ANALYSER CHANNEL NUMBER

Figure 6

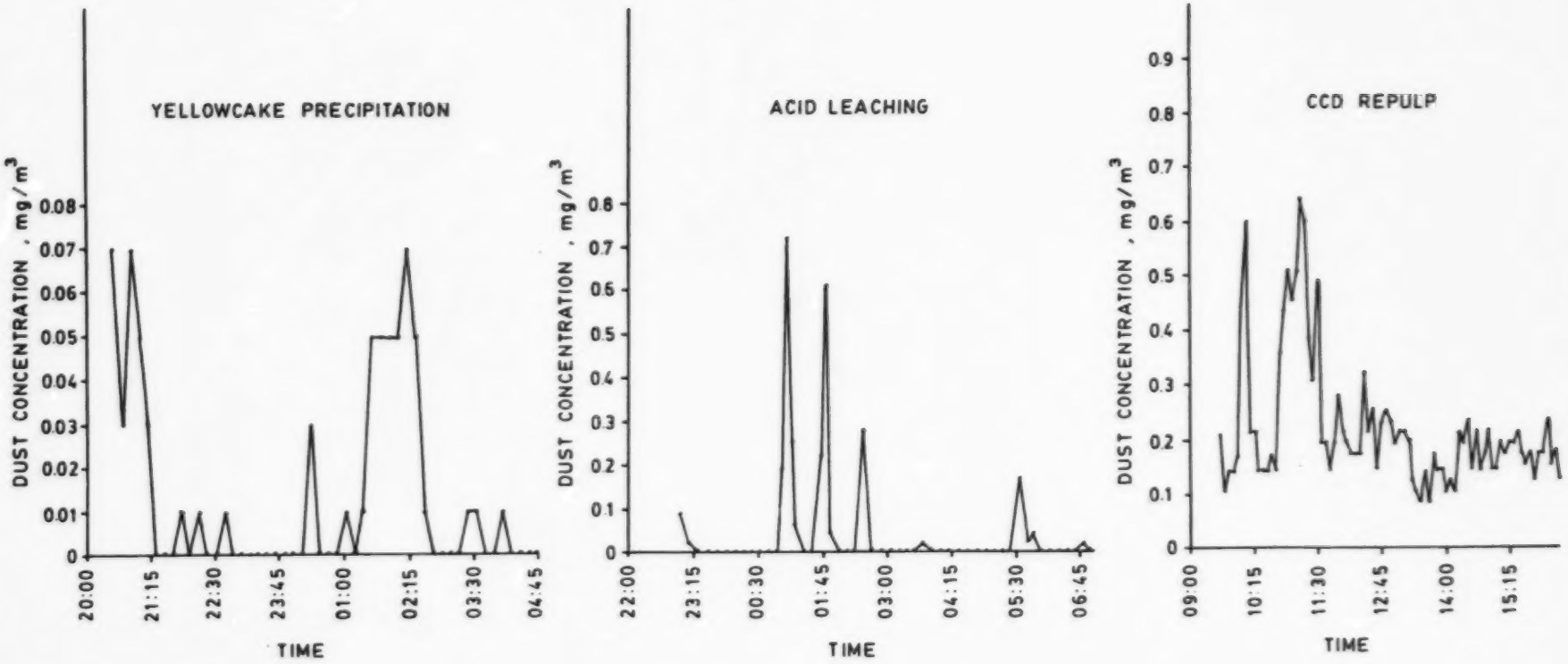
YELLOWCAKE PRECIPITATION
DUST CONCENTRATION , mg/m3
0
0.01
0.02
0.03
0.04
0.05
0.06
0.07
0.08
20:00
21:15
22:30
23:45
01:00
02:15
03:30
04:45
TIME
ACID LEACHING
DUST CONCENTRATION , mg/m3
0
0.1
0.2
0.3
0.4
0.5
0.6
0.7
0.8
22:00
23:15
00:30
01:45
03:00
04:15
05:30
06:45
TIME
CCD REPULP
DUST CONCENTRATION , mg/m3
0
0.1
0.2
0.3
0.4
0.5
0.6
0.7
0.8
0.9
09:00
10:15
11:30
12:45
14:00
15:15
TIME

Figure 7